Stallion Journal for Multidisciplinary Associated Research Studies
ISSN (Online): 2583-3340
Volume-3 Issue-4 || August 2024 || PP. 38-45 https://doi.org/10.55544/sjmars.3.4.5

Green Synthesis, Characterization and Study of Physical Properties of New Nanocomposite and Used as Adsorbent Surface and Photocatalyst for Waste Water Treatment

Afrah Hashim[1], Walaa Jubair Sabbar[2] and Entisar E. Al-Abodia[3]
[1,2]Directorate General of Education in Baghdad (Karkh1), Baghdad, IRAQ.
[3]College of Education Ibn Al-Haitham, Chemistry Department, University of Baghdad, Baghdad, IRAQ.

[3]Corresponding Author: aentisaree2000@gmail.com

www.sjmars.com || Vol. 3 No. 4 (2024): August Issue

Date of Submission: 25-07-2024	**Date of Acceptance:** 29-07-2024	**Date of Publication:** 29-08-2024

ABSTRACT

Article including, fabrication of a greatly effective catalyst consisting of ZnFG nanocomposite was studied using an in situ preparation method from specific weights of ZnO and iron oxide nanoparticles, as well as reduced graphene oxide. The effectiveness of fabricated composite as a photocatalytic surface was studied by applying it in advanced oxidation processes (AOP) to degrade methyl orange (MO) dye under sunlight. A high photodegradation efficiency of the dye was reached, about 85%, within 600 minutes. Photocatalysis experiments were conducted using multiple parameters such as time and temperature. The improvement in high photocatalytic activity of a prepared composite can be attributed to increased visible light absorption, reduced the band gap, and effective charge transfer between components. It was also observed that the ZnFG composite exhabited more stability even after repeated photocatalytic procedures, indicating repeated synergistic effects. It is possible that this kind of material can be applied as an efficient and stable photocatalyst for removing pollutants of various types.

Keywords- Green Synthesis, Waste Water Treatment, Catalyst, Photocatalyst.

I. INTRODUCTION

Dyes have long been used in several industries like plastics, cosmetics, textiles, dyeing, leather, papers, as well as food industry [1], which are caused environmental problems and clear hazards [2]. There are many classical methods of removing dyes such oxidation [3], adsorption [4-7], flocculation, membrane separation [8,9], coagulation [10], and photocatalys processes (advanced oxidation AOP) [11].

Photocatalyst methods have been widely studied for hazardous waste treatment and hydrogen production from water by renuble energy resources [12-16]. semiconductor materials like TiO2, MgO, ZnO, CdS, and WO3 can be utilized as photocatalytic agent, but some these materials are only active in the Ultra Violet area due to their big bandgap [13,17–19]. To develope the photocatalytic effectivness in the visible area, which encompasses about 45% of solar light, many of research have been conducted in order to increase the excitation wavelength region by lauding with another cations or anions [15-19].

Zinc oxide is one of the most promising materials for one-dimensional nanomaterial thats related to its potential implementations in optic, electronic, and photonic technology. This is revealed acceding to their characteristic properties like direct and wide band gap (about 3.36 eV) and large excitation correlation energy (about 60 meV). It crystallizes in two forms, hexagonal wurtzite as well as cubic zinc composite. Tetrahedral symmetry plays an essential role in the polarity of ZnO which arises along the hexagonal axis, it is considered the best one, that related to the high structural stability as well

as high photocatalytic effectiveness in removing different pollutants [17, 20]. ZnO nanostructures have many nanostructures, such as nanowires, nanobelts, nanosheets and nanorods, as well as hybrid composites [19-21]. Hollow spheres have gained great attraction due to their high photocatalytic efficiency, in addition to other advantages of this structure. Which is represented by the high surface area with low density in addition to the good surface permeability of these structures [20–22]. Many studies and research have been conducted on graphene, which is an extremely strong and highly conductive single-layer graphite sheet, for its use in multiple applications such as chemical sensors, supercapacitors, electronic and optoelectronic devices due to its exciting optical, electrical, thermal and mechanical properties [23-25]. Semiconducting inorganic nanostructures are typically hybridized onto graphene to fabricate graphene-based photocatalysts through a number of several approaches, most notably ex situ hybridization and in situ crystallization.

The former approach is known as the solution mixing method and involves mixing separate precursors containning graphene and other nanomaterials into the hybrid. Whereas, in the latter approach, simultaneous reduction is performed using an appropriate reduction method [26]. Moreover, several other methods have also been applied including thermal, hydrothermal, microwave, and others [27]. Utilizing these methods, a wide range of graphene-based semiconductor photocatalysts containing different nanoparticles such as ZnO, TiO2, SnO2, Cu2O, ZnS, CdSe, Bi2WO6, and CdS have been prepared [28].

Recently, magnetic nanoparticles (F3O4 MNPs) have received great interest in many fields due to their exceptional properties, such as their magnetic properties, large surface size relative to their volume, as well as plain surface conditioning potential. The high magnetic properties of nanostructures make dealing with them by applying an external magnetic field to them [29]. Therefore, in current study, a ZnFG nanocomposite was fabricated, appears promising as a photocatalyst for purifying polluted by decomposing industrial pollutants into green components, due to its small dimensions. The three components of the our composite (composed of various weights of rGO, F3O4, and ZnO). nanoparticles). The small dimensions lead to a large surface area for capturing BO dye in water under visible light irradiation due to the narrower band gap. Stretching in the excitation wavelength and decreased recombination of the photogenerated electron-hole pairs was confirmed by ultraviolet and visible (UV–Vis) spectra.

II. PRACTICAL PART

a. Preparation of nanomaterials and composites

The chemicals that were used in this work were supplied from Sigma-Aldrich Company and are of high purity. The Hammer method was used to prepare graphene oxide (GO) nanosheets [30] by oxidizing graphite using several oxidizing agents, namely concentrated H2SO4, NaNO3, and KMnO4. This is then followed by reduction of GO using hydrazine hydride to prepare graphene (G) nanosheets [31].

The green chemistry approach and the sol-gel method were used to prepare ZnONPs By adding 2000 mg of hydrated zinc nitrate with an amount of previously prepared plant extract, with continuous stirring, then placing it in a water bath at 60 °C for one hour, to obtain a liquid. It has a thick consistency. It is dried at 150 degrees Celsius for 4 hours and then burned at 400 degrees Celsius for one hour [32] The in situ preparation method was used to prepare the binary FG nanocomposite By co-deposition of iron(III) and(II) ions in a molar ratio of 2 to 1, in an alkaline conditions in the presence of reduced graphene oxide, while ZnFG was synthesized.

B. Photocatalytic efficiency

Photocatalytic reactions were carried out using sunlight as a source of ultraviolet radiation. During all photooxidation experiments for the decomposition of MO dye, at (298 K). Six samples containing (0.05 g) of fabricated composite (ZnFG) were with (50 ml) of a 20ppm MO solution (0.02 g of MO in 100 ml of distilled water), and placed in a water bath equipped with a Telg shaker. Its speed is about 100 r/min about 50 min to reach equilibrium state for adsorption (Figure 2).

Adsorption is the adhesion of liquid, gaseous, or solid molecules, known as adsorbents, to a solid or liquid surface, called an adsorbent. During this process, one or more layers of adsorbent material are created on the adsorbent surface. The adsorption process differs from other processes such as absorption, where the liquid is permeated or dissolved by a liquid or solid. If contact between the adsorbent and the adsorbent surface is maintained for a sufficient period, a balance will occur between the amounts of the adsorbed material on the surface and that present in the solution. In order to use the compound prepared in this study in the photocatalytic method, calculated time periods (50 minutes) were used to withdraw samples. And to isolate ZnFG molecules from MO solution by utilizing a magnetic field or a centrifuge. In order to known the amounts of MO dye remaining in the solution after each of sample withdrawal process, by utilizing Ultraviolet-visible spectroscopy at 465nm.

Stallion Journal for Multidisciplinary Associated Research Studies
ISSN (Online): 2583-3340
Volume-3 Issue-4 || August 2024 || PP. 38-45 https://doi.org/10.55544/sjmars.3.4.5

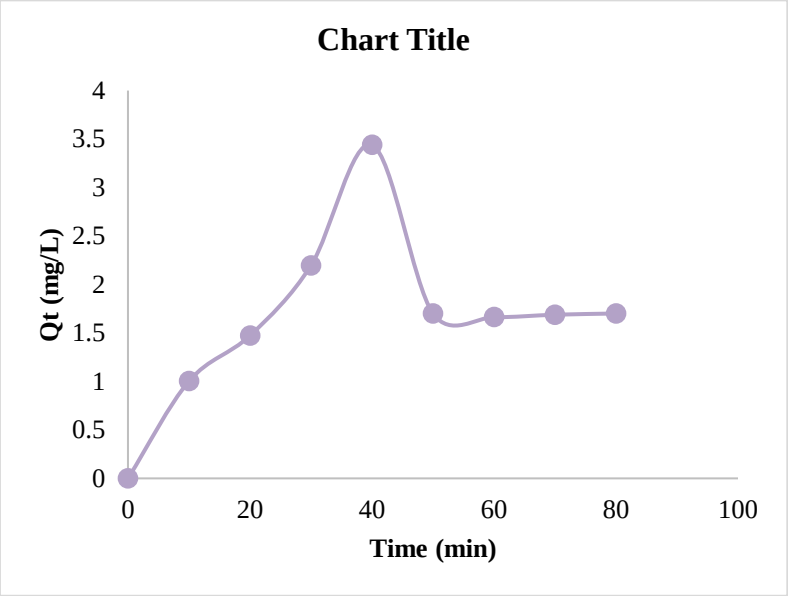

Figure 1. The equilibrium time of MO dye solution

III. RESULTS AND DISCUSSION

3.1. Infrared spectra analysis (FTIR)

To determine the effective functional aggregates and then characterize the materials and nanocomposites prepared in this study, using the Fourier-Transform Infrared Spectroscopy (FT-IR) technique. "Figure 2" gives the FTIR spectrum of the carbon nanomaterials prepared in this study, GO as well as G. We notice in Figure (2a), which represents the FTIR spectrum of graphene oxide, the broad peak at (3430 cm-1) that belongs to the stretching vibration of the hydroxyl group, and the two bands at (1620 cm-1 and 1722 cm-1) indicate on the stretching vibration of the (C = C) and (C = O) groups. The bands at (1362 cm −1 and 1226 cm −1) related to the stretching vibration of the acidic (CO) group and the alcoholic (C-OH) group, respectively. As for Figure (2b), which represents the FTIR spectrum of reduced graphene oxide (RGO), it shows the absence of the stretching vibration of the carbonyl group, and the appearance of a strong band at about 1604 cm-1, this is evidence of the recovery of the sp2 network and point to reducing GO [11,33].

Figure 3, which displays the FTIR spectrum of the plant extract OPE, notes the appearance of a broad peak attributed to the stretching of the O-H bond at 3286 cm. The C–H (CH2) bond stretching vibration is described by the peaks observed at 2921 and 2851 cm. C = Ostrich carbonyl stretching is observed at 1622 and 1645 cm. , while the C=O stretch resulting from carboxylic acid was found at 1417 cm −1. There is also the presence of C-O bending at 1089 cm and strong C = C bending vibrations[34]. The Figure (3b) of green ZnO is represents the FTIR spectrum, of a powder sample from a citrus peel extract which consider the initiated of Zink Oxide nanoparticles formation. The the strong broad band at 3378 cm^{-1} is corresponds to the hydroxyl OH group which commonly found in the most molecules linked on the surface of nanomaterials. The bands at 1560 cm-1, 1398 cm-1, 1040 cm-1 and 870 cm-1 are related to the following groups, stretching bending of carbonyl group COH (in-plane) , carboxylic acid vibrations as well as bending frequencies for C-O and –CH from the bending vibration (out-plane) for trans or E-alkene, respectively. (b) display the spectrum of ZnO NPs which showed a typical Zn-O extension at ~553 cm^{-1}[35,36]

The binary and ternary in the basic medium to precipitate magnetic iron oxide particles on the surface of graphene oxide (GO) to obtain the binary nanocomposite (FrGO), this indicates that the deposition process has occurred successfully and that the particles (Fe3O4MNPs), become completely superimposed with reduced graphene oxide (rGO), as it appeared in figure 4a, while figure 4b, repreasented the spectrum of rGO/Fe3O4/ZnO nanocomposite, it is clear that the C-O-C and C-O intensity peaks belonging to GO became weak or disappeared indicating that GO was reduced to rGO and mixing with Fe3O4 and ZnO to obtaind rGO/Fe3O4/ZnO nanocomposite [31]. the broad absorption at 3433 cm-1 is related to the stretching vibration of hydroxyl group. The absorption at 1618 cm-1 was assigned to the stretching vibration of the –C=C- of rGO. The absorption band at 567 cm-1 was due to Fe–O vibration. The peak at 471 cm-1 appeared identical to a Zn-O bond, which indicating the presence of ZnO. Figure (5) shown FESEM analysis of ZFrGO nanocomposite.

Stallion Journal for Multidisciplinary Associated Research Studies
ISSN (Online): 2583-3340
Volume-3 Issue-4 || August 2024 || PP. 38-45 https://doi.org/10.55544/sjmars.3.4.5

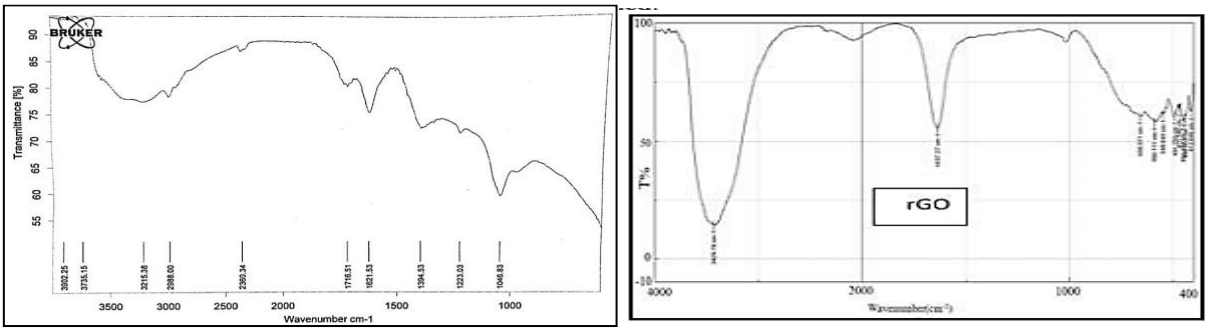

a **b**

Figure 2. FT-IR spectrum of (a) GO nanosheets and (b) G nanosheets

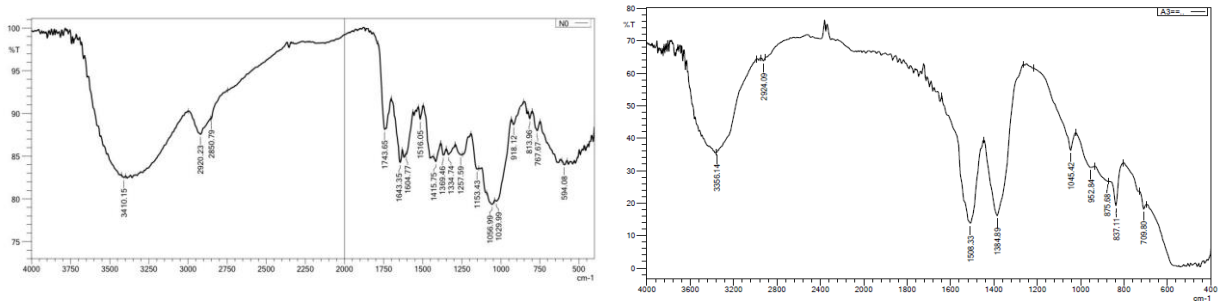

a **b**

Fig. (4-5). FTIR spectra a. orange peel extract, and b. Green ZnO NPs

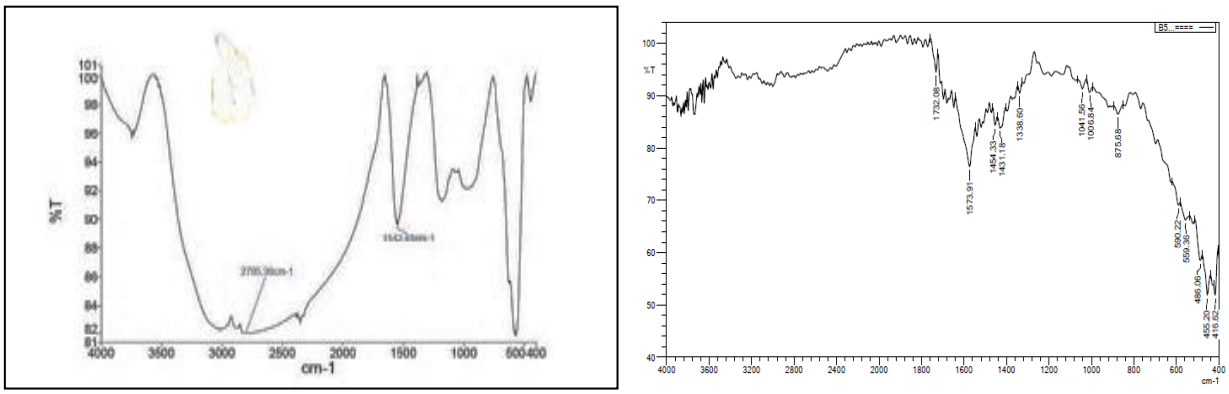

a **b**

Fig. (4). FTIR spectra a. FrGO and b. ZFrGO

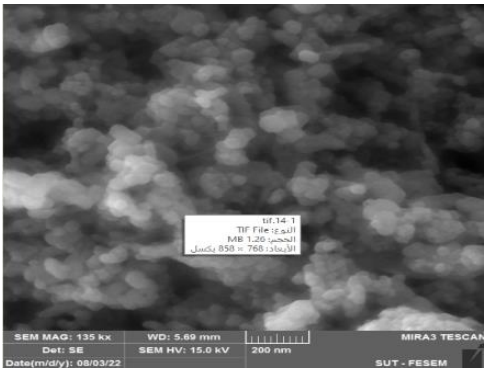

Figure (5): FESEM analysis of ZFrGO nanocomposite.

Stallion Journal for Multidisciplinary Associated Research Studies
ISSN (Online): 2583-3340
Volume-3 Issue-4 || August 2024 || PP. 38-45 https://doi.org/10.55544/sjmars.3.4.5

3.2. Efficient photodegradation

The photocatalytic activity of ZnFG nanocomposite as a photocatalytic agent was followed by determining the degradation speed of methyl orange (MO) dye dissolved in water. Heterogeneous catalytic oxidation involves a number of steps: (a) Diffusion and distribution of contaminants from the liquid phase on the surface of the ZnFG composite. (b) Adsorption of pollutants (dye molecules) on the surface of the ZnFG composite. (c) Oxidation and reduction processes occur. (d) Adsorption of products. (e) Removal of products from the interface area.

ZnO with a band gap of 3.2 eV has been frequently used in photocatalytic applications. The remaining amount of MO dye in the reaction mixture was calculated using a spectrophotometer. The photocatalytic mechanism of ZnFG nanocomposite in the presence of solar radiation can take the following steps: [37,38].

$ZnO + h\nu \rightarrow ZnO\ (e^-_{(CB)}) + (h^+_{(VB)})$ (1)
$ZnO(h^+_{(VB)}) + H_2O \rightarrow ZnO + H^+ + {}^\bullet OH$ (2)
$ZnO(h^+_{(VB)}) + OH^- \rightarrow ZnO + {}^\bullet OH$ (3)
$ZnO(e^-_{(CB)}) + O_2 \rightarrow ZnO + O_2^{\bullet -}$ (4)
$O_2^{\bullet -} + H^+ \rightarrow HO_2^\bullet$ (5)
$HO_2^\bullet + HO_2^\bullet \rightarrow H_2O_2 + O_2$ (6)
$ZnO\ (e^-_{(CB)}) + H_2O_2 \rightarrow {}^\bullet OH + OH^-$ (7)
$H_2O_2 + O_2^{\bullet -} \rightarrow {}^\bullet OH + OH^- + O_2$ (8)
$H_2O_2 + h\nu \rightarrow 2{}^\bullet OH$ (9)
${}^\bullet OH + R \rightarrow$ Intermediates $\rightarrow CO_2 + H_2O$ (10)

Where VB and CB represent the valence and conduction bands, respectively, hv is the excitation energy [eg]. The above equations are shown in Figure 6, which represents a scheme of photodegradation of MO dye by ZnFG compound under sunlight illumination. The results acquired for MO dye decomposition are shown in Table 1. Ultraviolet–visible spectroscopy of MO dye solution at varying times, and at main band λ_{max} = 465 nm.

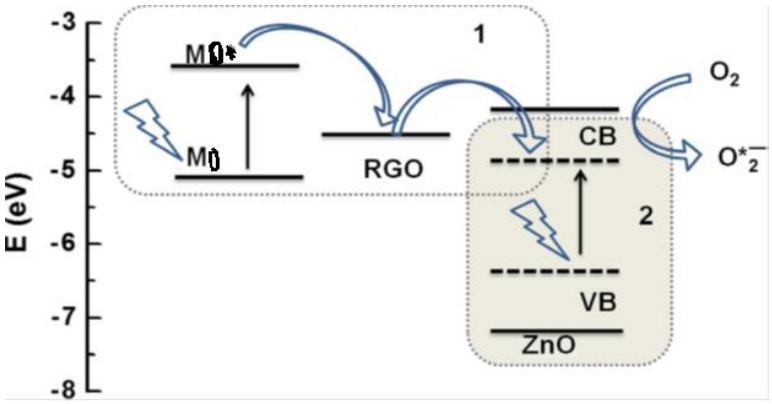

Figure 6. Scheme of photodegradation of MO dye by ZnFG compound under sunlight illumination [38].

Photocatalytic process experiments were conducted at different photocatalytic effects such as times and temperatures. The absorption variation of MO solution at varying parameters in the presence of ZnFG nanocomposite was studied using UV-Vis spectroscopy.

The removal efficiency (R%) of ZnFG composite was determined by utilizing equation 12[39].

$$R\% = \frac{C_o - C_t}{C_o} \times 100 \qquad (12)$$

C_t and C_o were the final and initial amounts of MO solution, results Inserted in table 1.

Table 1: Photocatalytic results of ZnFG nanocomposite as Photocatalysis agent.

T(min)	T(298K)			T(299K)			T(309K)		
	C_t	C_t/C_0	R%	C_t	C_t/C_0	R%	C_t	C_t/C_0	R%
-50	10.55	1	0	10.55	1	0	10.55	1	0
0	10.24	0.971	2.887	9.89	0.937	6.255	9.61	0.911	8.902

Stallion Journal for Multidisciplinary Associated Research Studies
ISSN (Online): 2583-3340
Volume-3 Issue-4 || August 2024 || PP. 38-45 https://doi.org/10.55544/sjmars.3.4.5

120	8.735	0.828	17.2	8.037	0.762	23.82	7.415	0.703	29.71
240	7.999	0.758	24.18	7.161	0.679	32.12	6.298	0.597	40.3
360	6.565	0.622	37.77	5.753	0.545	45.47	5.346	0.507	49.32
480	4.877	0.462	53.77	4.534	0.43	57.02	3.684	0.349	65.08
600	4.039	0.383	61.71	2.288	0.217	78.31	1.819	0.172	82.76

The photocatalytic activities of ZnFG were found by calculating the decomposition rate of methyl orange (MO) dissolved in water. Figure 7a, b and c show the time profiles of the dye degradation using the main absorption peak of MO (465 nm) under visible light irradiation at various temperatures. As shown in the figure, ZnFG sample showed a significant improvement in the photocatalytic activity over time, as it is noted from the figures mentioned that the increase in MO dye dissolution increases significantly with time progression until it reaches about 80% at the 600th minute, as well It is noted that the increase in the dissolution of the dye increases with increasing temperatures, as we find that the percentage of dissolution of the dye per minute 600 reaches about 85% at a temperature of 309 K, while it is equal to 61% at a temperature of 289 K, and this is due to the increase in temperatures It leads to an increase in the kinetic energy of the molecules, which leads to an increase in collisions between them, and thus to an increase in the photooxidation process and the decomposition of the MO dye.

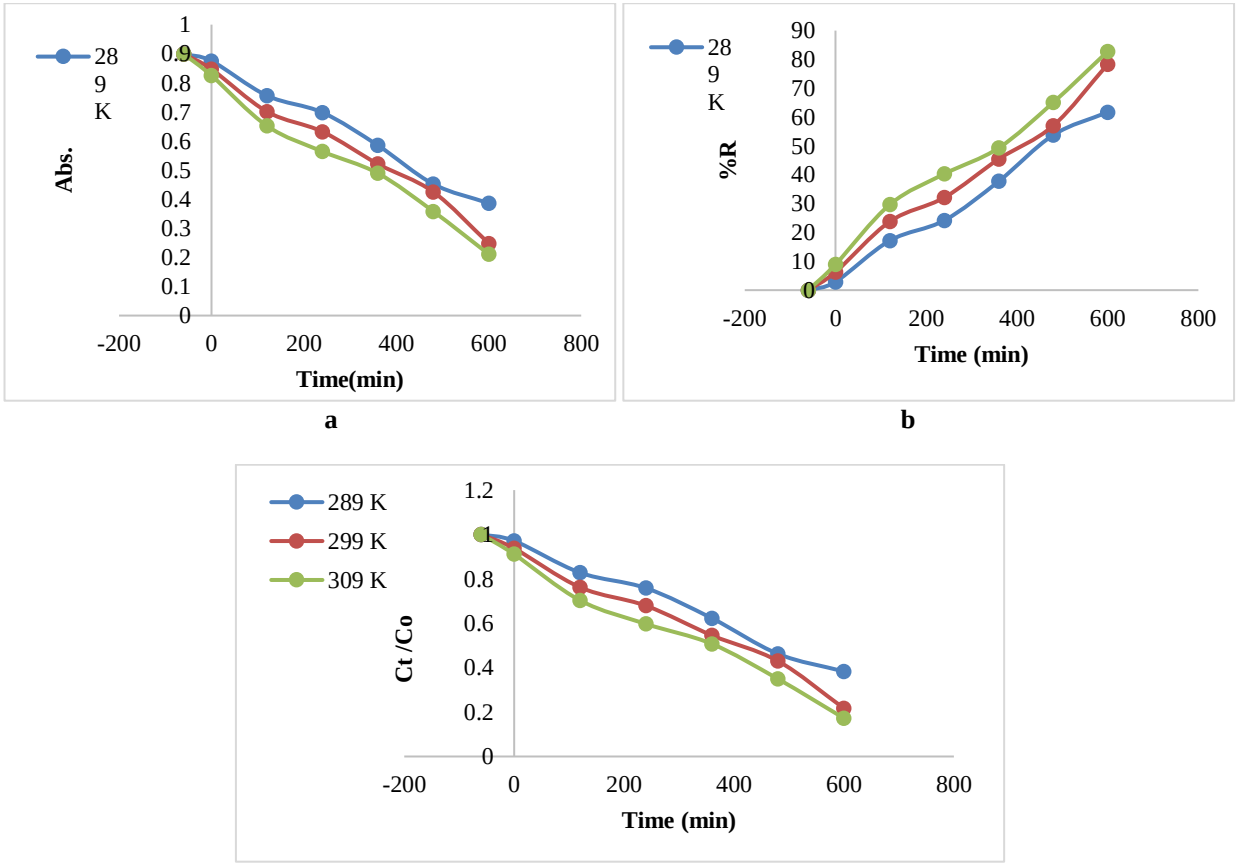

Figure 7. Photooxidation of MO dye in the presence of ZnFG composite as a photooxidation agent at varying temperatures..

IV. CONCLUSION

Aim of our study is to describe the ZnFG nanocomposite prepared from mixing known amounts of GO nanosheets and Fe3O4 and ZnO nanoparticles. The green chemistry approach and the sol-gel method were used to prepare ZnONPs. The effectiveness of the prepared ternary composite as an AD photocatalyst was studied in (AOP) for the decomposition of MO dye in its aqueous solutions under sunlight. It was found that the removal efficiency of MO dye reached 98% when utilizing ZnFG composite as a catalyst within 120 min.

REFERENCES

[1] R. Maas, & S. Chaudhari, Biochem. 40, 699–705 (2005).
[2] T. Plaztek, C. Lang, G. Grohmann, U. S. Gi & W. Baltes, Hum. Exp. Toxicol. 18, 552–559 (1999).
[3] H. Nourmoradi, S. Zabihollahi, & H. R. Pourzamani, Desalin. Water Treat 57, 5200–5211 (2015).
[4] L. Musab, and E. E. Al- Abodi , Energy Procedea 157(2019) 752-762.
[5] A.Jawad and E.E. Alabodi " Investigating (Fe3O4) Magnatic Nanoparticles Impregnated onto Tri-sodium citrate to Remove, of methylene blue dye from Aqueous Solutions", AIP Conference Proceedings 2123, 020026 (2019).
[6] H. A.J. Almuslamawy, R. A. Hashim, A. H. Aldhrub and R. S. Mouhamad "Biosorption of Pollutants in Diyala River by Using Irrigated Vegetables" Asian Journal of Water, Environment and Pollution, Vol. 20, No. 2 (2023), pp. 31-37.
[7] Almuslamawy, H. A.J., Aldhrub, A. H., S. Ali, Mouhamad, R. S. "Microbial Simultaneous Eradication from Wastewater of Sulphate and Heavy Metals". Asian Journal of Water, Environment and Pollution, vol. 20, no. 3, pp. 85-90, 2023
[8] R. M. Kadhim, E. E. Al- Abodi, and A. F. Al-Alawy, Iraqi Patent No. B01D61/005 C02F1/445(2017).
[9] R. M. Kadhim, E. E. Al-Abodi, and A. F. Al-Alawy, Desalination and Water Treatment 115 45–52 (2018)
[10] A. K. Verma, R. R. Dash & P. Bhunia, J. Environ. Manage. 93, 154–168 (2012).
[11] Y.M.Sadiq, and E. E. Al- Abodi "Preparation and Characterization of Anew Nano Mixture and Its Application as Photocatalysis in Self-Assembly Method for Water Treatment", AIP Conference Proceedings 2190, 020042 (2019).
[12] L. Lin, Y. Yang, L. Men, X. Wang, D. He, Y. Chai, B. Zhao, S. Ghoshroy, Q. Tang, Ahighly efficient TiO2@ZnO n–p–n heterojunction nanorod photocatalyst, Nanoscale 5 (2013) 588–593.
[13] J.S. Lee, K.H. You, C.B. Park, Highly photoactive, low bandgap TiO2 nanoparticles wrapped by graphene, Adv. Mater. 24 (2012) 1084–1088.
[14] T.-D. Nguyen-Phan, V.H. Pham, E.W. Shin, H.-D. Pham, S. Kim, J.S. Chung, E.J. Kim, S.H. Hur, The role of graphene oxide content on the adsorption-enhanced photocatalysis of titanium dioxide/graphene oxide composites, Chem. Eng. J. 170 (2011) 226–232.
[15] X. An, J.C. Yu, Graphene-based photocatalytic composites, RSC Adv. 1 (2011) 1426–1434.
[16] Q. Xiang, J. Yu, M. Jaroniec, Graphene-based semiconductor photocatalysts, Chem. Soc. Rev. 41 (2012) 782–796.
[17] Y. Liu, Y. Hu, M. Zhou, H. Qian, X. Hu, Microwave-assisted non-aqueous route to deposit well-dispersed ZnO nanocrystals on reduced graphene oxide sheets with improved photoactivity for the decolorization of dyes under visible light, Appl. Catal. B 125 (2012) 425–431.
[18] S. Anandan, N. Ohashi, M. Miyauchi, ZnO-based visible-light photocatalyst: Band-gap engineering and multi-electron reduction by co-catalyst, Appl. Catal. B 100 (2010) 502–509.
[19] S. Cho, J.-W. Jang, J. Kim, J.S. Lee, W. Choi, K.-H. Lee, Three-dimensional Type II ZnO/ZnSe heterostructures and their visible light photocatalytic activities, Langmuir 27 (2011) 10243–10250.
[20] J. Yu, X. Yu, Hydrothermal synthesis and photocatalytic activity of zinc oxide hollow spheres, Environ. Sci. Technol. 42 (2008) 4902–4907.
[21] K. Matsuyama, K. Mishima, T. Kato, K. Ohara, Preparation of hollow ZnO microspheres using poly(methyl methacrylate) as a template with supercritical CO2-ethanol solution, Ind. Eng. Chem. Res. 49 (2010) 8510–8517.
[22] Q.-P. Luo, X.-Y. Yu, B.-X. Lei, H.-Y. Chen, D.-B. Kuang, C.-Y. Su, Reduced graphene Oxide–hierarchical ZnO hollow sphere composites with enhanced photocurrent and photocatalytic activity, J. Phys. Chem. C 116 (2012) 8111–8117.
[23] V.H. Luan, H.N. Tien, T.V. Cuong, B.-S. Kong, J.S. Chung, E.J. Kim, S.H. Hur, Novel conductive epoxy composites composed of 2-D chemically reduced grapheme and 1-D silver nanowire hybrid fillers, J. Mater. Chem. 22 (2012) 8649–8653.
[24] M.J. Allen, V.C. Tung, R.B. Kaner, Honeycomb carbon: a review of graphene, Chem. Rev. 110 (2009) 132–145.
[25] A.K. Geim, K.S. Novoselov, The rise of graphene, Nat. Mater. 6 (2007) 183–191.
[26] M. Khan, M.N. Tahir, S.F. Adil, et al, Graphene based metal and metal oxide nanocomposites: synthesis, properties and their applications, J. Mater. Chem. A 3 (2015) 18753–18808.
[27] A. Madni, S. Noreen, I. Maqbool, et al, Graphene-based nanocomposites: synthesis and their theranostic applications, J. Drug Target. 26 (2018) 858–883.
[28] T.A. Saleh, G. Fadillah, Recent trends in the design of chemical sensors based on graphene–metal oxide nanocomposites for the analysis of toxic species and biomolecules, TrAC, Trends Anal. Chem. 120 (2019) 115660.
[29] P. Christian, F. Von der Kammer, M. Baalousha and T.h. Hofmann, Nanoparticles: structure, properties, preparation and behavior in environmental media, Ecotoxicology, 17 326-343(2008).
[30] Hummers W S and Offeman R E, 1958, J. Am. Chem. Soc. 80 1339.

[31] Park S, An J, Potts J R, Velamakanni A, Murali S and Ruoff R S 2011 Carbon 49 3019.
[32] HI, T. U. D., NGUYEN, T. T., THI, Y. D., THI, K. H. T., PHAN, B. T. & PHAM, K. N. 2020. Green synthesis of ZnO nanoparticles using orange fruit peel extract for antibacterial activities. RSC advances, 10, 23899-23907.
[33] N. Jabbar, (2023)" Antimicrobial Activity and physical and mechanical properties of Dental Materials with and without the Nanoparticles and plant extracts". M.Sc. Thesis, The college of College of Education Ibn Al-Haytham for Pure Sciences–University of Baghdad, Iraq.
[34] ZAPATA, B., BALMASEDA, J., FREGOSO-ISRAEL, E. & TORRES-GARCIA, E. 2009. Thermo-kinetics study of orange peel in air. Journal of thermal analysis and calorimetry, 98, 309-315.
[35] P. A. Luque, *et al.*, Green synthesis of zinc oxide nanoparticles using Citrus sinensis extract, *J. Mater. Sci. Mater. Electron.*, 2018, **29**(12), 9764–9770.
[36] Tu Uyen Doan Thi,†ab Trung Thoai Nguyen,†ab Y Dang Thi,c Kieu Hanh Ta Thi,ab Bach Thang Phanbc and Kim Ngoc Pham, Green synthesis of ZnO nanoparticles using orange fruit peel extract for antibacterial activities, RSC Adv., 2020, 10, 23899.
[37] K. Nejati, Z. Rezvani & R. Pakizevand, Synthesis of ZnO nanoparticles and investigation of the ionic template effect on their size and shape. Int. Nano Lett. 1(2): 75-81(2011).
[38] D. Rajamanickam & M. Shanthi , Photocatalytic degradation of an organic pollutant by zinc oxide – solar process. Arab J Chem 9:S1858–S1868(2016). http:// dx.doi.org/10.1016/ j.arabjc.2012.05.006.
[39] M. A. Rauf & S. S. Ashraf, Fundamental principles and application of heterogeneous photocatalytic degradation of dyes in solution. Chem. Eng. J.;151:10–8(2009). http:// dx.doi.org/10.1016/j.cej.2009.02.026.